HADLEY CENTRE TECHNICAL NOTE NO. 8

SIMULATING CLIMATIC CHANGE OF THE SOUTHERN ASIAN MONSOON USING A NESTED REGIONAL CLIMATE MODEL (HadRM2)

By

D Hassell and R Jones

May 1999

Hadley Centre for Climate Prediction and Research
Meteorological Office
London Road
Bracknell
Berkshire RG12 2SY

NOTE: This paper has not been published. Permission to quote from it should be obtained from the Director of the Hadley Centre.

Contents

Abstract

Simulations of the response to climate change of the Indian monsoon using a regional climate model (RCM) are presented. Twenty year simulations of current climate and the climate of 2041–2060 assuming a 1% compound increase of CO_2 are assessed. Comparisons between the driving GCM and RCM control simulations and climatology show that the models capture the main features of the large scale flow. During the Indian monsoon season the RCM simulates a more realistic distribution of precipitation and improved spatial detail in the surface climatology in general. The RCM also provides a more realistic distribution of the break and active regimes of the monsoon and captures associated regional detail over southern India with superior skill, correctly simulating increased precipitation over southern India during break events.

There are large responses to increased CO_2 in the surface climatology of the models despite small changes in the mean flow. The semi-permanent heat low over north west India and Pakistan is seen to intensify and, in the GCM, shift position. In general, changes are qualitatively consistent between the two models, e.g. a reduction in soil moisture over India, with maxima in north west and in to Pakistan. However, large fine scale differences are also apparent, a 60% increase in precipitation in flood prone Bangladesh the GCM being reduced to 20% in the RCM. This is still significant, however, and the greater skill of the RCM control simulation lends much more credibility to such a predictions. The active/break cycle is seen to intensify, and in particular in the RCM the mean break precipitation departure from the long term mean diminishes over southern India. The RCM's response in this aspect appears to have a higher level of attributable skill than its driving model, as the reliability of the GCM response is questionable due to poor behaviour in its control.

1 Introduction

The agronomics of much of southern and eastern Asia is intrinsically linked with the annual monsoon cycle. It is also a major factor in the severity of the periodic flooding of Bangladesh and surrounding low lying areas. An understanding of the behaviour of the monsoon is thus an essential part of economic planning, disaster mitigation and developing adaptation strategies to cope with climate variability and possible climate change. The major impact of the monsoon is via the temporal and spatial variability of its precipitation which in turn are controlled by complex interactions of atmospheric physics and dynamics. These are most comprehensively modelled using atmospheric general circulation models (GCMs) though computational limitations restrict their spatial resolution. In order to overcome this limitation we use a higher resolution regional climate model (RCM) for the Indian monsoon region which is driven by output from a GCM.

There have been many studies of the Asian monsoon using GCMs (e.g. Meehl and Washington (1993), Bhaskaran *et al.* (1995),Chakraborty and Lal (1994), Goswami (1998)) which simulate the large-scale flow well though they generally have less success with observed summer rainfall distributions. This is unsurprising, with typical gridlengths of at least 400km even with perfect simulation of the mean flow only broad features will be captured. However, to model impacts of climate variability or change much finer spatial detail is required. One approach is to use a nested RCM (e.g. Giorgi (1990)), as has been developed at the Hadley Centre (Jones *et al.* (1995)). This 50km grid model has been adapted for studies over the monsoon region by Bhaskaran *et al.* (1996, 1998). They find that the RCM provides realistic simulations of both time averaged features and intraseasonal variability of the monsoon, whilst also capturing important regional detail not resolved by its driving GCM.

In this article we present the first investigation into the response to climate change over the Indian monsoon region using a regional climate model. Boundary conditions are provided by a coupled ocean-atmosphere GCM which has been demonstrated to provide a good simulation of the mean monsoon circulation and has shown to have some skill at capturing observed precipitation, temperature and interannual variability over the Indian subcontinent (Bhaskaran and Mitchell, 1998). This was integrated to provide simulations of the current climate and a climate responding to increasing CO_2 concentrations. Boundary conditions from these simulations were

then used to drive a RCM (derived from the atmospheric component of the GCM) designed to improve the simulation of regional climate by representing mesoscale forcings and circulations not resolved by the GCM. A brief description of the models and this experimental design follows. The control climates are then compared with climatology (section 3) including detailed investigation of the break and active monsoon regimes. The response in the surface climatology is then investigated (section 4) and finally preliminary conclusions and areas for further investigation are identified (section 5).

2 The models and experimental design

The general circulation model (GCM) used in this report is the second Hadley Centre coupled ocean-atmosphere GCM (HadCM2) (Johns *et al.*, 1997). The RCM (HadRM2) is a high resolution limited area atmosphere model driven at its lateral and sea surface boundaries by output archived from a previous HadCM2 integration. The formulation of HadRM2 is identical to the atmospheric component of HadCM2, apart from details concerning diffusion and filtering. Both models use 19 hybrid coordinate vertical levels and regular latitude-longitude horizontal grids. The grid spacing in HadCM2 is $2.5° \times 3.75°$ and $0.44° \times 0.44°$ in HadRM2 which is kept quasi-regular over the region of interest by shifting the coordinate pole. The timesteps are 30 and 5 minutes respectively. General details of the RCM formulation and the one-way nesting technique may be found in Jones *et al.* (1995). The choice of integration domain (e.g. fig. 1) has been shown to exhibit no significant restrictions in mesoscale circulation when compared with two larger domains whilst requiring less computer time (Bhaskaran *et al.* (1996), their RCM3 domain). The atmospheric component of the GCM used by Bhaskaran *et al.* (1996, 1998), is a slightly modified version (HadAM2a) than that used in the present study, having improved precipitation and cloud schemes and changes to the horizontal diffusion characteristics.

Control and perturbed GCM simulations have each been carried out for 21 years. Atmospheric CO_2 is held constant in the control simulation at the present day value. The scenario for the perturbed integration (GHG) has observed increases in CO_2 from 1860–1990 and thereafter compound increases of 1% per year. The GHG integration was initialized after 50 years of compound increases, in the year 2040. The nested RCM simulations were integrated over the same periods with the first year disregarded. This report concentrates on the mean climate change over 20 years (equivalent to 2041–2060) in the anomaly integrations, as well as looking at interannual and intraseasonal aspects of precipitation and large-scale flow.

3 Control climate

3.1 Mean general circulation

Mean atmospheric circulations in boreal summer (JJA) are validated by comparison with the new 15 year ECMWF re-analysis (ERA) (Gibson *et al.*, 1997).

In JJA, both models simulate well the mean position of the monsoon trough as seen in geopotential height fields at 850 hPa (fig. 1) although it is too broad and penetrates too far into the Bay of Bengal. The pattern of flow over the Arabian sea through to the Bay of Bengal is also well captured. The Mascarene high, intraseasonal anomalies in which have been linked to monsoon intensity (Pant and Rupa Kumar, 1997), is well simulated in the driving GCM, in both magnitude and position (fig. 2). As a result, the Somali jet is reasonably well positioned in the horizontal (fig. 2) (and also the vertical, not shown), though the jet core west of the Somali coast extends too far over the Arabian sea consistent with sharper pressure gradients to the north of the Mascarene high. Flow coming in to the west of the RCM domain in both models is too strong (fig. 1), consistent with the overestimation of the Somali jet, but the penetration into the Bay of Bengal is weaker in the RCM, probably due to the enhanced orographic elevation of

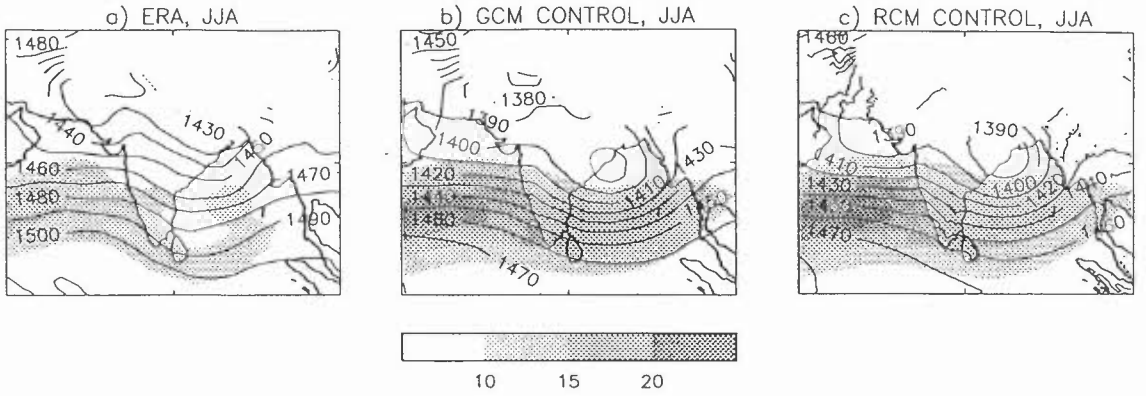

Figure 1: JJA Geopotential height (m, contoured) and isotachs (ms^{-1}, shaded) at 850 hPa. a) ERA data averaged from 1979-93, b) GCM control 20 year average and c) RCM control 20 year average.

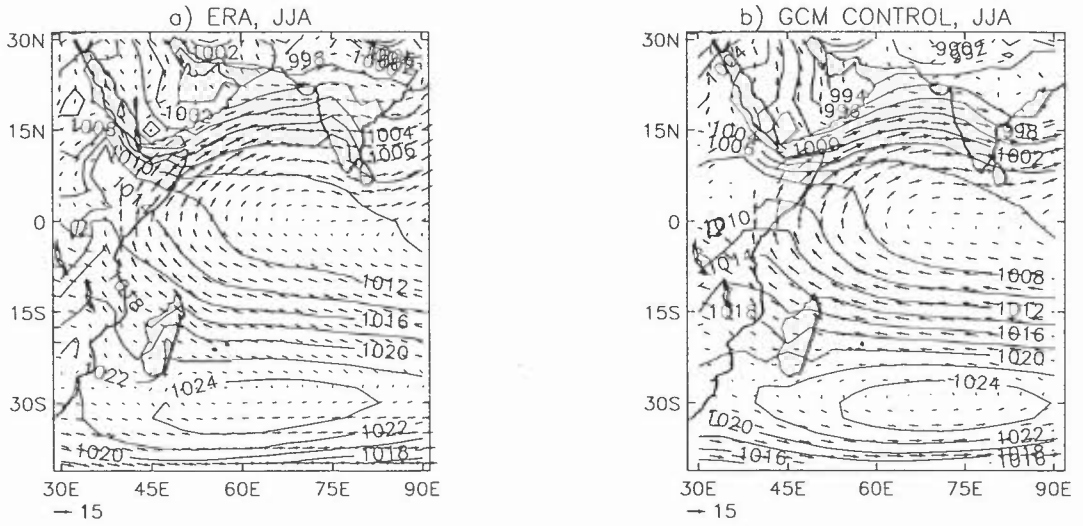

Figure 2: Pressure at mean sea level (hPa) and wind vectors (ms^{-1}) at 850 hPa for JJA. a) ERA data averaged from 1979-93 and b) GCM control 20 year average.

the Western Ghats acting as a barrier.

Dominant upper tropospheric easterlies over the Indian peninsula and westerlies north of the Himalayas are well captured in both models (fig. 3). Both models correctly position the easterly jet in both latitude and height (not shown), although the models over estimate the upper level divergence around the Tibetan anticyclone is consistent with an over active monsoon trough (see section 3.3).

3.2 Mean surface climate

To assess the simulated monsoon season (June to September, JJAS) rainfall distributions, three gridded precipitation climatologies are considered: CMAP (Xie and Arkin, 1997), LW (Legates and Willmott, 1990) and CRU (New *et al.*, 1997), also giving a range of other surface variables). CMAP is a blend of uncorrected gauge data and satellite observations whereas the LW and CRU (precipitation) datasets utilize only terrestrial station sources, the gauge data of the latter being uncorrected for gauge-induced biases. The climatologies agree in their synoptic patterns over the domain, but show significant mesoscale differences (fig. 4). Gridded rainfall climatologies are recognized to exhibit such differences (Stephenson *et al.*, 1998), and information may be lost during interpolation in areas with strong spatial heterogeneities (Pant and Rupa Kumar, 1997). In particular, the data in areas of monsoon rainfall clearly show large variability in

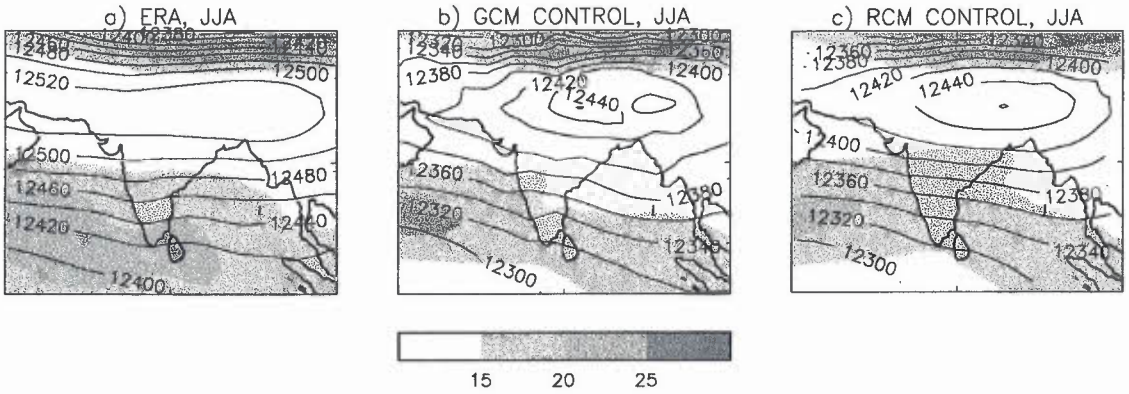

Figure 3: JJA Geopotential height (m, contoured) and isotachs (ms^{-1}, shaded) at 200 hPa. a) ERA data averaged from 1979-93, b) GCM control 20 year average and c) RCM control 20 year average.

their intensities, and so all three climatologies will be considered. The observed pattern of precipitation maxima on the western side of the Western Ghats, the Burmese side of the Bay of Bengal and the Himalayan upslopes is captured in both models (fig. 5), as are the dry deserts of Iran and Afghanistan. Evidence from other mountainous regions (e.g. the Alps, Frei and Shär (1998)) suggest that the high mean precipitation over the Himalayan upslopes seen in LW is realistic. These maxima in the GCM are similar to the observed magnitudes, but are larger in the RCM. The observed rain-shadow zone over the southern tip of the Indian peninsula and Sri Lanka is only seen in the RCM. The minimum of precipitation in the RCM seen in the Himalayas, towards the western end of the ridge, is seen partially in the LW climatology, but is not clear in either the GCM or the CMAP and CRU climatologies.

Between the two models, area averaged summer surface air temperatures over sea, land and the whole domain are within 0.5 K of each other. Compared to the CRU gridded surface

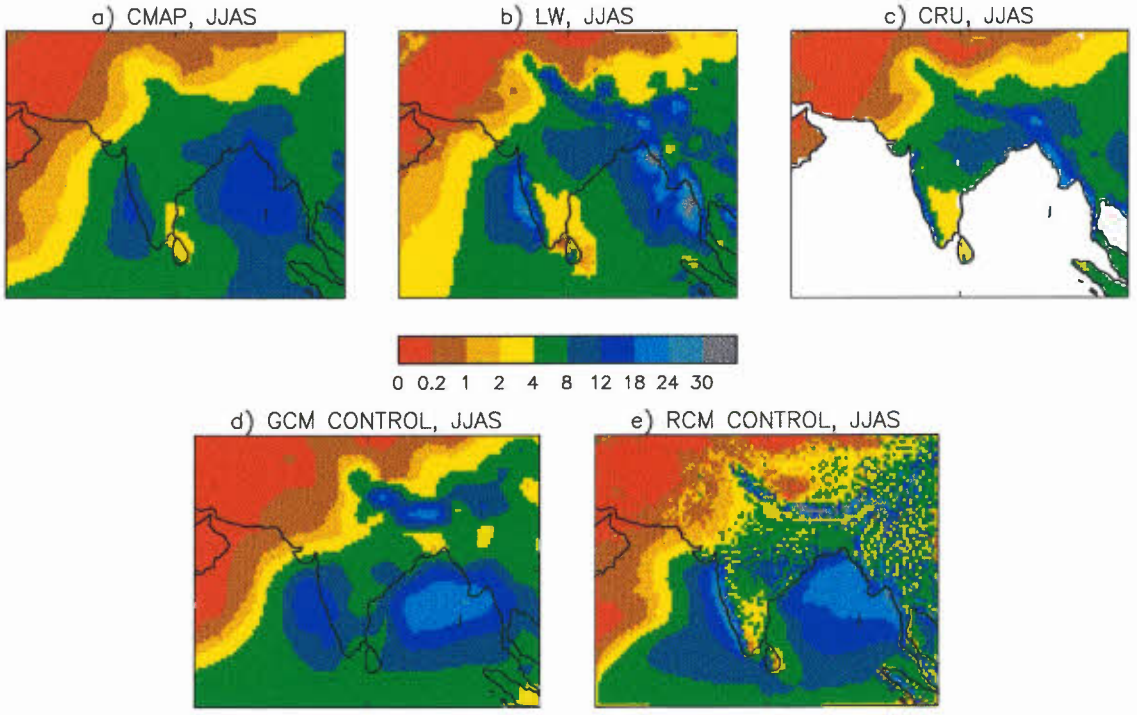

Figure 4: Simulated precipitation distributions for June to September (mm/day). Observed precipitation distributions for June to September (mm/day), see text. a) CMAP climatology, b) LW climatology and c) CRU land climatology 1961-90. d) GCM 20 year average and be RCM 20 year average.

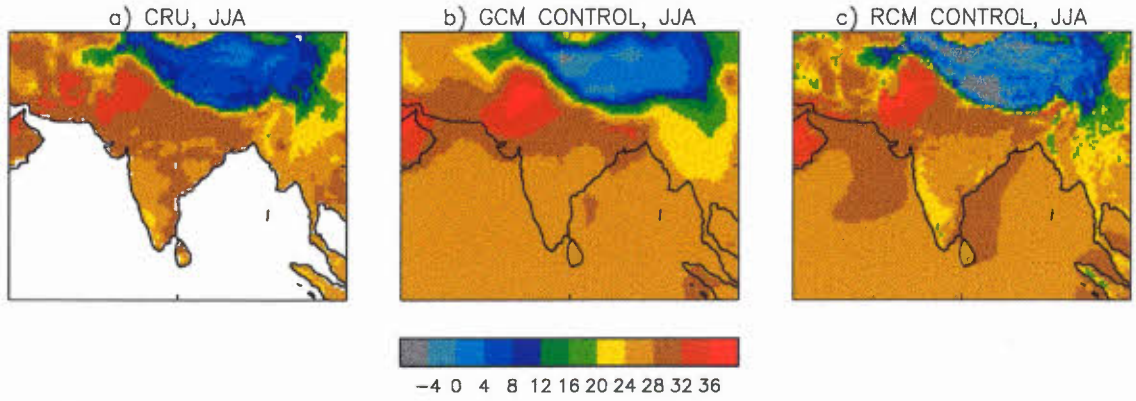

Figure 5: Mean surface air temperature (°C) for JJA. a) CRU land climatology 1961-90, b) GCM 20 year average and c) RCM 20 year average.

climatology for 1961-1990 (New *et al.*, 1997), both models capture the large-scale distribution well (centred pattern correlations of 0.95 (GCM), 0.96 (RCM)) (fig. 6) with land area averaged means agreeing within 0.5 K. Both models exhibit a larger spatial temperature range, especially in areas of extreme mean temperature (upper regions of the Himalayas, parts of Pakistan). The RCM also displays considerable spatial detail over the GCM when comparing with the CRU data. In particular, the GCM does not capture notably cooler areas over the Western Ghats (where the maximum RCM and CRU elevations are twice as high as in the GCM). The surface temperature maximum (and associated heat low) over north eastern India and Pakistan is correctly positioned in both models, but extends too far towards the south west in the GCM. Much of the southern area of the Tibetan plateau is $\sim$ 10 K cooler than CRU. This could be due to excessive areal snow cover in higher areas (Johns *et al.*, 1997) as a result of unrealistic numerical diffusion of moisture up steep slopes.

3.3 Monsoon season variability

The normal monsoon onset date in central India is the same in each model (not shown). This is 11 days later than estimated from observations (IMD, 1943), comparable with other HadCM2 experiments (Bhaskaran and Mitchell, 1998).

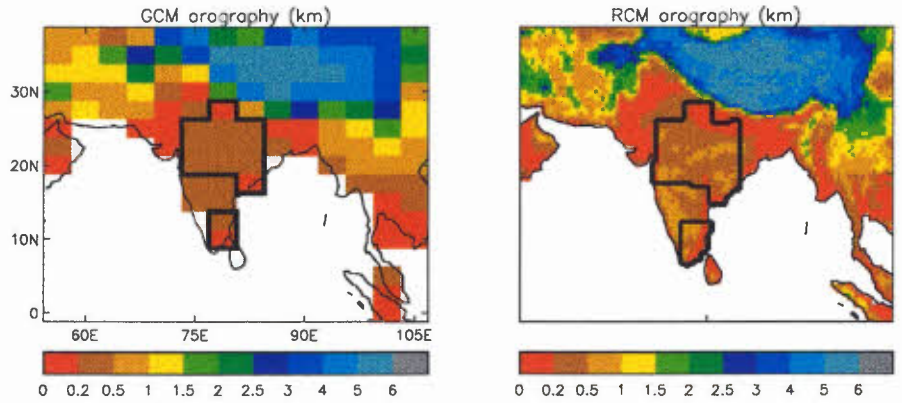

Figure 6: Model orographies (km). Also shown are the representations of the central Indian states of Madhya Pradesh and Vidarbha and the southern Indian state of Tamil Nadu (see text). a) GCM (regular latitude-longitude grid) and b) RCM (rotated coordinate pole).

The intraseasonal variability of the models is considered by looking at the behaviour of the active/break monsoon cycle, in particular the frequency, duration and large scale nature of these climatic regimes.

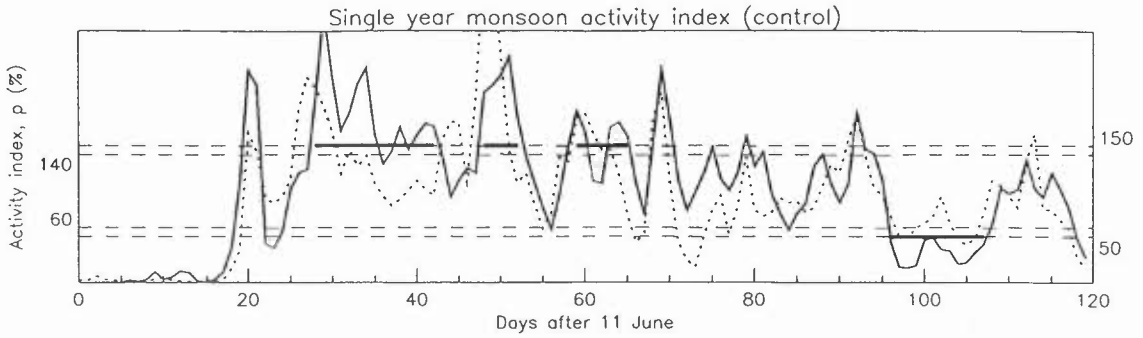

Figure 7: An example (6th year of integration) of the monsoon activity index (p) diagnosed from each model. Solid = GCM, dotted = RCM. The thicker solid horizontal lines indicate where active and break periods have been identified in the GCM.

Following an observed climatology of monsoon activity for 1967–83 derived by Alekseeva *et al.* (1989), the Indian Meteorological Service's criteria for classifying break and active periods is adopted. Daily monsoon activity, p, is measured as the precipitation percentage of the long term mean daily precipitation averaged over the central Indian states of Madhya Pradesh and Vidarbha. The climatology utilized 29 rain gauges in this area, and considered 1st June – 30th September as the monsoon season. Days are classified according to $p < 50\%$ (break) and $p > 150\%$ (active). These definitions were adapted for use with the models as follows:

1. The central Indian states are approximated with 11 GCM grid boxes and 464 corresponding RCM points (fig. 6).

2. A distinct period of activity lasts at least three days (Hamilton, 1979) and is at least three days away from a period of the same activity.

3. The p value thresholds for active and break days are 140% and 60% respectively, reflecting an estimated 10% error in daily rain gauge measurements (Legates and Willmott, 1990). This prevents active and break periods starting or ending due to small departures of the activity index across the thresholds (fig. 7). The thick horizontal lines in this figure show where the GCM's active and break periods have been identified.

4. The four month monsoon season is shifted to begin on 11th June to account for the delay in the GCM's simulated normal monsoon onset.

Data source	No. of periods		Regime days		Mean length		Tamil Nadu		
	Break	Active	Break (%)	Active (%)	Break (days)	Active (days)	Full (mm/day)	Break (%)	Active (%)
Obs	36	31	20.2	12.4	11.6	8.3	4.10	—	—
Con GCM	32	52	8.5	15.4	6.7	7.5	8.46	92	107
Con RCM	33	49	8.8	9.6	6.8	4.3	3.94	110	77
GHG GCM	41	66	15.0	24.8	8.8	9.0	8.61	100	109
GHG RCM	51	66	14.9	15.5	7.0	5.7	3.90	102	82

Table 1: Columns 1 and 2: Number of active/break periods identified in each 20 year simulation, and the 17 years climatology (Alekseeva *et al.* 1989). Columns 3 and 4: Mean percentage of days in each season falling into break and active categories. Columns 5 and 6: Mean length of break and active periods. Column 7: Mean precipitation over Tamil Nadu. The observational value is the mean of the three climatologies in figure 4. Columns 8 and 9: Model active/break precipitation rates over Tamil Nadu given as a percentage of the full seasonal mean.

In an average monsoon season the mean number of break periods per season is well captured by both models (table 1) though they overestimate the number of active periods by 40%.

Data source	No. of periods		Regime days (%)		Mean length (days)	
	Break	Active	Break	Active	Break	Active
Con GCM	35	60	8.5	16.2	5.8	6.5
Con RCM	30	56	8.4	11.6	6.7	5.0

Table 2: As table 1 columns 1 to 6, but for the band pass filtered monsoon activity time series (control only).

However, both models severely underestimate the mean break period length i.e. these events are broken down too rapidly. The mean number of days spent in the active phase compared to the observations differs widely (+25% (GCM), −25% (RCM)). Though with the increased numbers of simulated active periods this implies that mean active regime lengths are underestimated in both models, and more so in the RCM.

Calculating the model's variability on time scales of 2 to 6 days may help to attribute causes behind the differing active and break characteristics. This time scale was chosen to encompass the minimum length of active and break periods. Figure 8 shows the 2 to 6 day variability in simulated and observed (ERA) daily 1000 hPa geopotential height fields, calculated using Blackmon's band pass filter (Blackmon, 1976). The general level in the RCM is seen to compare well with the climatology (e.g. the 7 metre contour) whereas the GCM underestimates the variability throughout the domain and tends to be more zonally symmetric. The RCM has the additional feature of a much larger maximum in the monsoon trough region which may result from an increased number and/or increased intensity of cyclones in the monsoon trough. The RCM grid (50km) will resolve cyclones better than ERA (150km) and the GCM (400km) and is sufficiently fine to capture typhoons.

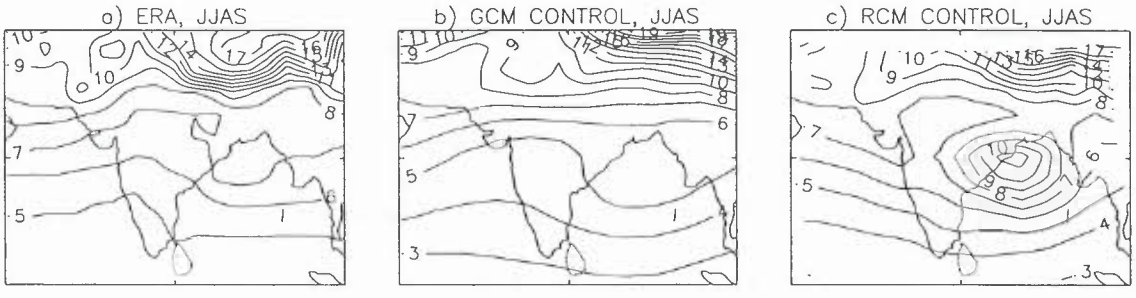

Figure 8: Standard deviation of 2 to 6 day band-pass filtered 1000 hPa geopotential height (m) fields for JJAS. a) ERA data averaged over 1979-93, b) GCM control averaged over 20 years and c) RCM control averaged over 20 years.

To see how the differing patterns of variance affect the models' break and active regimes, 2 to 6 day variability was removed from the monsoon activity time series (p) and active and break days recalculated. Compared with table 1, the both filtered activity time series show a +15% increase in the number of active periods, 20% increase in the amount of RCM active days but a much smaller +5% change in the GCM. Both models display negligible changes in their break characteristics. So, the greatly differing model variability does not explain the the break phase deficiencies (similar in the both models) but suggests that higher levels of variability, especially in the monsoon trough region, may influence breaking down of active regimes.

The frequencies at which a given number of active or break periods occur in a season are shown in fig. 9. It is clear that the models do not reproduce the observed distribution. However, the observations are only a small sample and they lie within the envelope of a representative set of GCM samples. This envelope demonstrates the variability in the model on timescales of greater than 10 years, as is seen generally in the observational record. An example of observed interdecadal variability is the link between the the all India rain index (AIRI), normalized by its standard deviation, and the southern oscillation index (SOI). Between 1951 and 1972, the seven El Niño warm events are associated with below normal rainfall for the season preceding

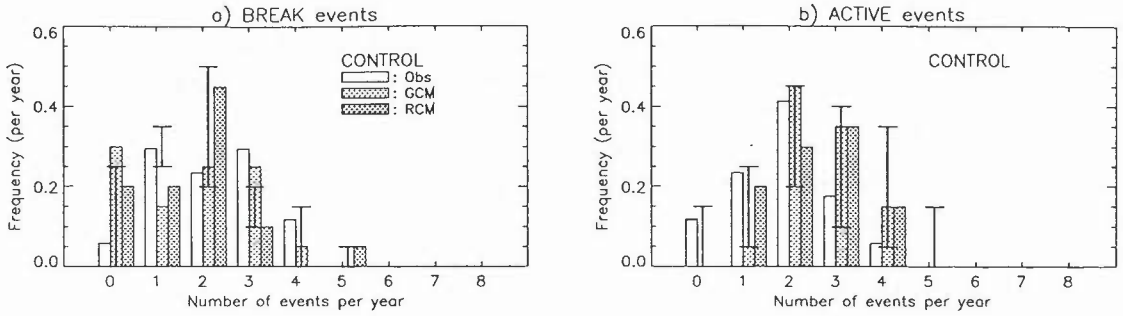

Figure 9: Frequency distribution of the observed (Alekseeva *et al.* 1989) and simulated number of occurrences of break and active periods per year. The overlaid bars indicate the range of values in each bin from seven 20 year periods chosen at random from 600 years of a parallel HadCM2 control integration (the present integration not included.

the peak warming and above normal rainfall during the following season. However, during the three warm events of 1982–1991 the Nino 3 sea surface temperature (SST) anomalies are seen to change phase (peaking in January as opposed to November) and monsoon rainfall is seen to be deficient after, as well as before, an El Niño event (Webster *et al.*, 1998).

Sensitivity tests have shown that the predicted numbers of break and active periods are highly dependent on the exact nature of the criteria used to define them. This problem may only be overcome by applying the same criteria to both observed and modelled daily precipitation time series, thus ensuring a 'like with like' comparison. At present such daily data is unavailable.

Composited winds at 850 hPa

The behaviour of the models in active and break regimes may be analyzed by forming composites of model variables over all relevant days and comparing them with full mean (averages

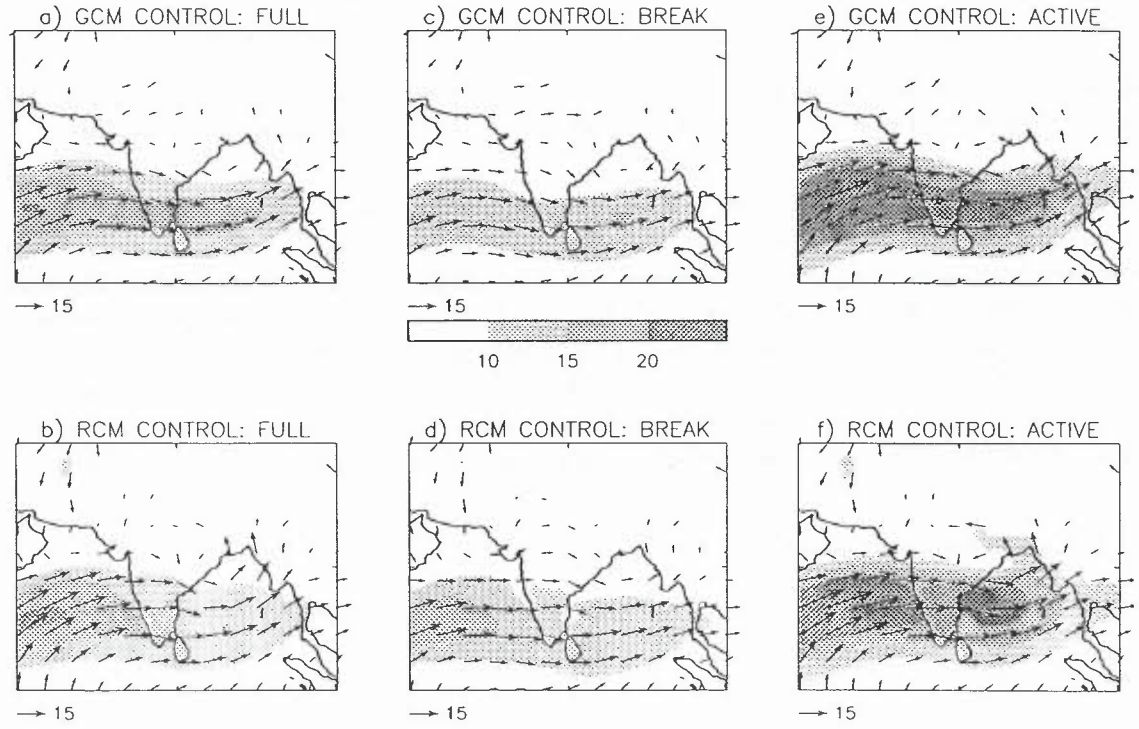

Figure 10: Simulated GCM and RCM control monsoon season wind vectors and isotachs (ms^{-1}, shaded) at 850 hPa. a) and b) Full 20 year seasonal mean, c) and d) Break regime composite, e) and f) Active regime composite.

over all monsoon season days: 11th June – 10th October). During break conditions, the low level jet core at 850 hPa over the Arabian sea is observed to weaken and turn anticyclonically, thus passing over the southern tip of India. The monsoon trough also fills or shifts northwards over the Himalayan foothills. Flow during active regimes is characterized by a strengthening of the westerlies over central India and a deepening of the monsoon trough (Annamalai *et al.*, 1998). It has been suggested (Rodwell, 1997) that advection into the region of air with significant negative potential vorticity may be responsible for the an anticyclonic turning during break phases. As a consequence, this mechanism may trigger some breaks in the monsoon by altering the moisture fluxes entering the region.

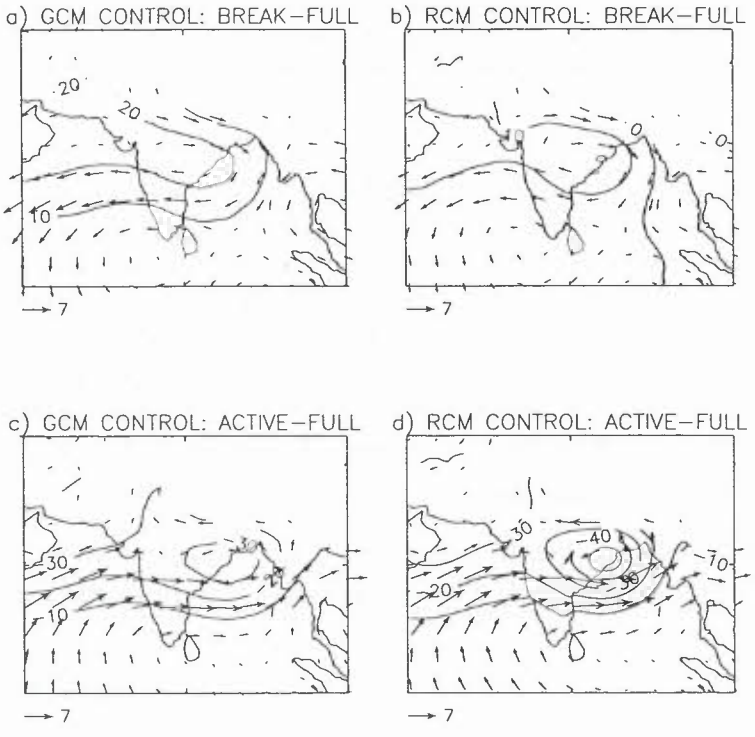

Figure 11: Simulated GCM and RCM control break and active 850 hPa wind vector and geopotential height (m) anomalies. a) and b) Full mean minus break composite, c) and d) Full mean minus active composite.

Both model break composites of 850 hPa flow clearly show a filling of the trough and a weakening of the jet core in comparison to the full mean (figs. 10, 11). The anticyclonic turning over Southern India is a secondary feature, but is certainly present in each model. The modelled active composite flows also capture the observed features, in particular the deepening of the monsoon trough. Whilst the RCM and GCM results are qualitatively similar, compared to the GCM the RCM break composite shows a slightly diminished departure from the full mean and an enhanced active phase departure (particularly a greater deepening of the monsoon trough). This validation of the large-scale flow climatologies is a good indication that the break and active regimes have been correctly diagnosed.

Composited precipitation

The observed spatial differences between typical active and break precipitation regimes may be characterized (Hamilton, 1977) by the mean break minus active anomalous precipitation rate as a percentage of the full mean (fig. 12). Positive percentages indicate greater precipitation rates during break periods than during active phases and vice versa for negative values. Here we consider the southern Indian state of Tamil Nadu as well as north east India and Bangladesh, as the nature of the precipitation in these areas is independent of the criteria used for diagnosing active and break days. Hamilton reports percentages of greater than 50% over these areas with

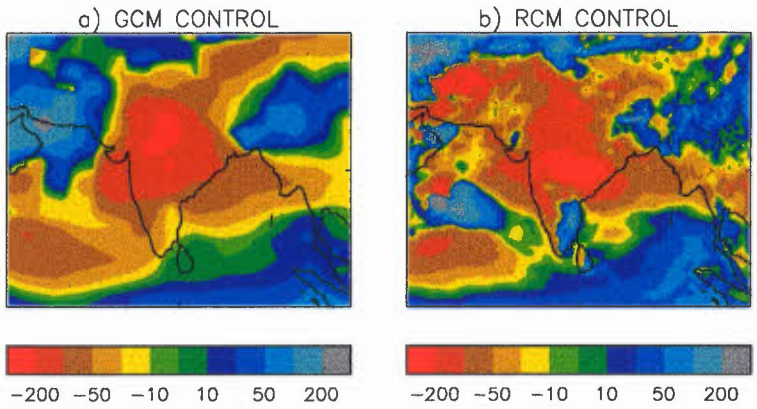

Figure 12: Relative characteristics of break and active precipitation composites. Each field is the difference in break and active composite precipitation as a percentage of the full mean. a) Control GCM, b) Control RCM

values less than −50% over much of central India.

The large negative percentages over central India in both models (fig. 12) are to be expected within the current definition of break and active days. Only the RCM captures all of the observed behaviour over southern India described above. The GCM exhibits an erroneous reversal, i.e. more precipitation during active periods than break periods (table 1). The poor GCM behaviour is probably related to its highly overestimated full mean precipitation. In turn, this may be linked to the unrealistically strong low level jet strength (fig. 1) and the GCM's lack of orographic modulation of the moisture fluxes (not shown). As a consequence, little skill can be attributed to precipitation information from the global model over the south of India. Over NE India and Bangladesh in the RCM, the small area of greater active precipitation to the east of Bangladesh is probably due to orographic forcing by the Ganges valley, a topographic feature not present in the GCM.

In conclusion, these simulations have some deficiencies in their active and break regimes statistics, in particular breaks are too short. However, typical large-scale flow and patterns during each regime compare well with observed behaviour though the associated precipitation patterns are only captured in the RCM.

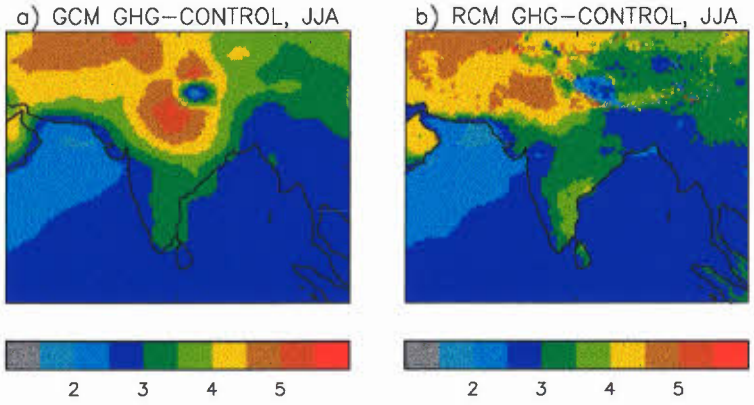

Figure 13: Simulated surface air temperature anomaly (K) for JJA. a) GCM: GHG minus control 20 year average and b) RCM: GHG minus control 20 year average.

4 Response to increasing CO_2

4.1 Mean surface climate

On increasing greenhouse gases, SSTs in JJA increase everywhere with a region average of +2.1 K (fig. 13). Warming is largest over the south Arabian Sea and the northern half of the Bay of Bengal, with minima occurring off the coast of Pakistan and east of Indonesia. Over land, there is also warming everywhere, with an area average of 2.5 K in each model. Surface air temperature change over the western India is spatially similar between models, and the relatively small land/sea temperature contrast suggests that increases over land are modulated by warmer westerlies over the Arabian sea. There are, however, notable differences over south eastern India, a secondary surface temperature maximum in the RCM; and northern India, a larger warming in the GCM with a maximum of 5.5 K at 80°E near the foot of the Himalayas.

The GCM maximum corresponds to an expansion towards the south east of the semi-permanent heat low (Bhaskaran *et al.*, 1995). This feature is not as intense and does not extend as far south in the RCM which is probably more realistic. In the GCM control there is an erroneous south easterly extension of the surface temperature maximum along with lower precipitation (fig. 4) and soil moisture (not shown). This implies a greater tendency for a positive feedback on temperature brought about by soil drying early in the season followed by reduced evaporation from the surface, which artificially enhances the GCM response in the warmer climate. The intensification of the heat low coincides, as expected, with decreases over the same area in summer season soil moisture content (70%) and evaporation (50%). The magnitude of the minimum in PMSL lying over the heat low increases and shifts accordingly to the south east, thus also strengthening 10 metre winds around the depression.

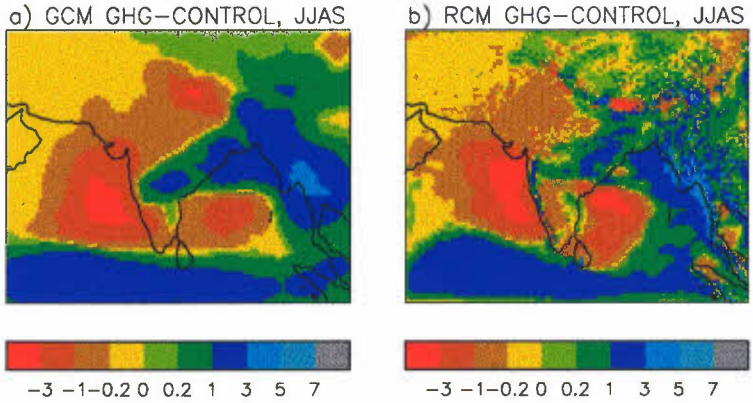

Figure 14: Precipitation anomaly (mm/day) for JJAS. a) GCM: GHG minus control, b) RCM: GHG minus control.

Summer mean precipitation exhibits a complex pattern of increases and decreases (fig. 14). Increases are seen over the southern Indian ocean and over land in the eastern half of the domain. Around the Bay of Bengal, the RCM displays considerable spatial detail in the pattern of precipitation change not in the GCM, including relatively sharp land/sea contrasts. The north western deserts see a small decrease in the absolute amount of rainfall, but the largest reductions over land are seen over northern India, where large reductions in soil moisture and evaporation also occur. Increases are seen over the entire area encompassing Bangladesh and Burma, as well as the eastern side of India. However, the larger response in the GCM is suspect due to its underprediction of mean precipitation over these areas in the control climate (fig. 4).

Changes in soil moisture (fig. 15) approximately follow those in precipitation except in central eastern India where they decrease due to enhanced drainage from the soil (not shown). Largest reductions are seen in the arid regions with reductions of 60% (and mean precipitation reduced to < 1 mm/day) over north west India and Pakistan, an effect clearly linked to the surface

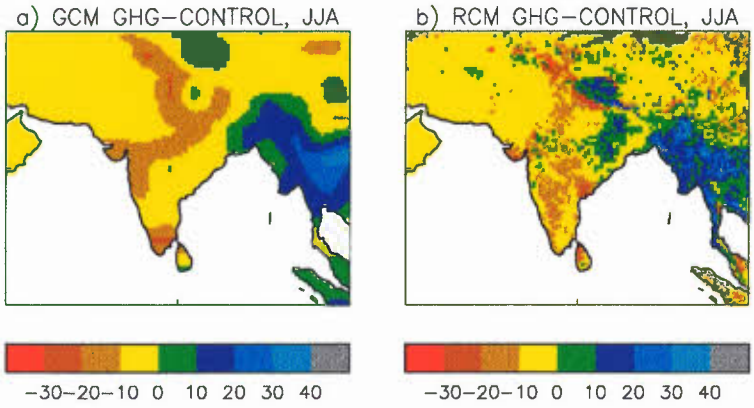

Figure 15: Anomalous soil moisture content (mm) for JJA. a) GCM: GHG minus control, b) RCM: GHG minus control.

temperature response. In the GCM, large increases are seen over Bangladesh, where precipitation increases by more than 60% locally and soil moisture content almost doubles. Similar, although less extreme behaviour is exhibited by the RCM, in which the position of maximum increase is situated over north eastern India, due to smaller precipitation increases. The RCM response is more believable, again due the shortcomings of the control GCM's precipitation.

4.2 Monsoon dynamics and variability

Under the GHG scenario, the normal model onset dates are approximately 7 days (GCM) and 13 days (RCM) later than the control. The GCM behaviour is consistent with previous work (Bhaskaran and Mitchell, 1998), but the mechanisms behind the extra shift in the RCM onset date are not clear at present.

The large–scale circulation responses in JJA at 850 and 200 hPa are small (not shown), although there is a northern shift and weakening of the low level jet core over the Arabian sea (fig. 17 c.f. fig. 10). This could be influenced by the reduced meridional SST gradient apparent in these areas (figs. 5, 13). The mean position and intensity of the upper level Tibetan high is unchanged. Monsoon precipitation activity has been linked with fluctuations in the pressure difference (ΔP) between the Mascarene high and the monsoon trough (Cadet, 1983); large positive ΔP being indicative of strong (active) monsoon periods. The global model predicts a mean increase in ΔP of 3 hPa under climate change, suggesting an enhancement in either intensity, frequency or longevity of active phases of the monsoon.

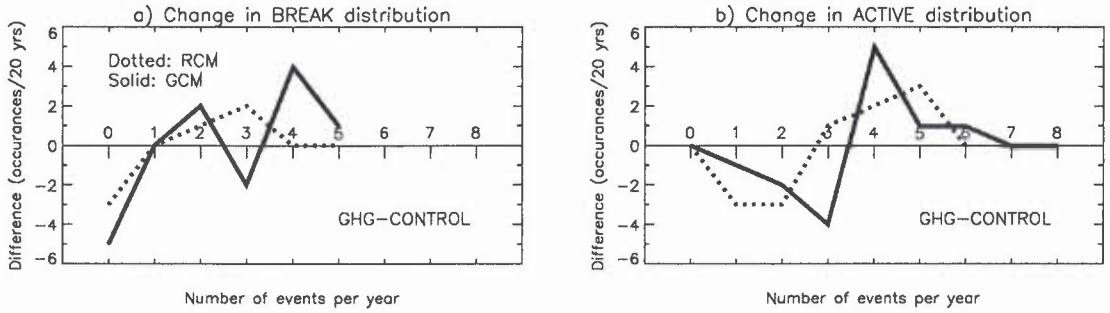

Figure 16: Change under increasing CO_2 of the distribution of simulated number of occurrences of break and active periods per year (c.f. fig. 9). Differences are given as the anomalous number of occurrences in the full 20 year integration.

The mean number and length of active and break periods increases (table 1), the RCM increase in number of break periods being 50% higher than in the GCM. Figure 16 shows that

both break and active frequency distributions become skewed towards more years with higher numbers of each type of activity. The nature of changes in the active distributions are similar in each model, with the mean active period length increasing by 30%.

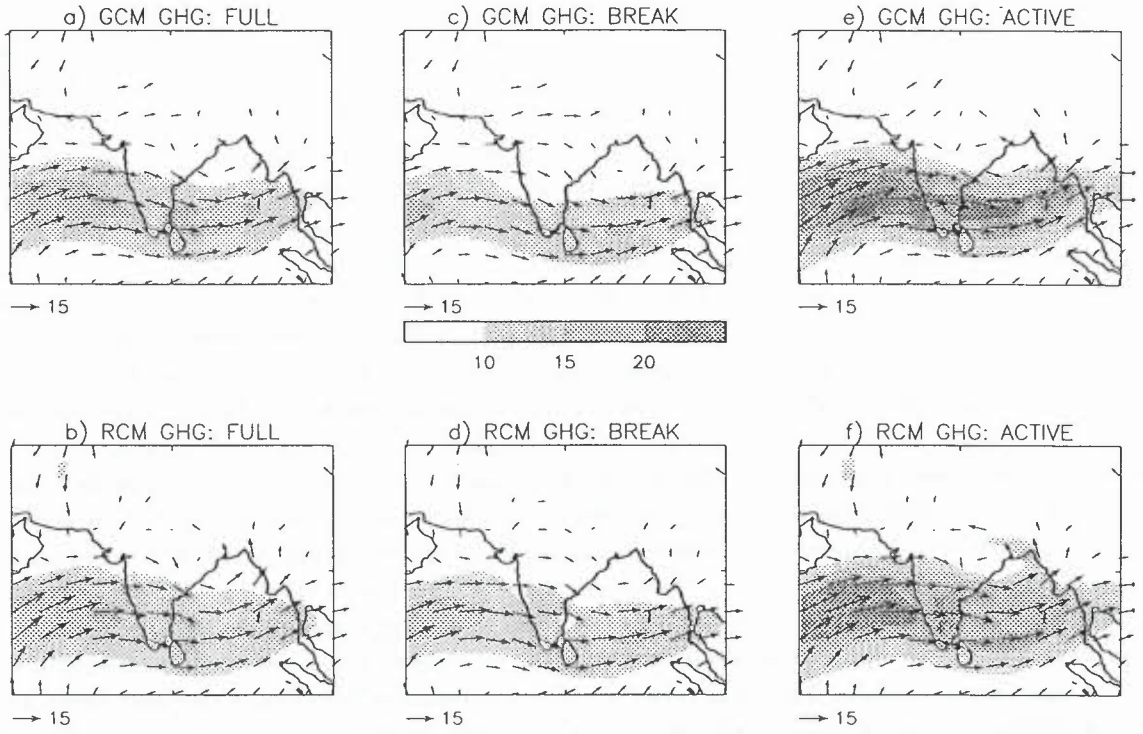

Figure 17: Simulated GHG monsoon season wind vectors and isotachs (ms^{-1}, shaded) at 850 hPa. a) and b) Full 20 year seasonal mean, c) and d) Break regime composite, e) and f) Active regime composite.

During break conditions, the anticyclonic turning of the jet over the Arabian sea is more pronounced in both models (fig. 17 c.f. fig. 10), but the reduction in strength from the full mean is diminished, by a factor of two in the RCM. The increase in jet strength during active phases is also reduced, as is the deepening of the monsoon trough. The RCM still shows larger differences from the full mean than the GCM and both models exhibit similar patterns of the relative conditions between active and break precipitation composites to those seen in the control simulations. The relationships between the composites and their corresponding full mean have, however, altered. Whilst mean RCM break rainfall over Tamil Nadu is greater than the long term average in the control, it is now indiscernable from the full mean as might be expected from the GHG break flow behaviour. The result is the same in the GCM, although the response is in the opposite direction (break precipitation being augmented to the full mean rate). The coincidence between break precipitation over southern India and circulation both becoming akin to the full mean situation may only be seen to be meaningful in the RCM case, as the GCM responses are masked by systematic errors in the control simulation (section 3.3).

Whilst the mechanisms involved in the different behaviour of the models have not been fully investigated at present, we believe that the responses are more realistic in the RCM given its better simulation of active and break regimes.

5 Summary and concluding remarks

The control GCM provides a good simulation of the mean climate of the south Asian monsoon though it fails to capture some local details of the surface climate. The position of the monsoon trough, lower and upper level jets are well simulated as are the broad features of the surface temperature and precipitation. Upper level divergence, however, is overestimated, coincident

with an over-deep monsoon trough. The regional model reproduces the large-scale features of the GCM climate and adds realistic local detail. The deflection of the low level flow over south India, the rain shadowing of the western Ghats and the extent of the north Indian surface temperature maximum are all closer to observations.

Analysis of the break and active phases of the monsoon, important intraseasonal variations, have again shown that both models capture many relevant features with the regional model having greater skill locally. The number of break periods is well captured, though they are too short lived, but numbers of active periods are overestimated. The spatial patterns of composites of low level flow in each regime compares well with the SHIVA climatology (Annamalai *et al.*, 1998) indicating that the models are reproducing the observed dynamics within these regimes. Composites of precipitation, however, show that only the regional model is able to capture observed local details of its spatial variation with the regimes.

Under increasing atmospheric CO_2 concentrations, changes in the mean synoptic flow are small. However, mean surface temperatures are seen to increase everywhere with a maximum increase over north India. This is weaker and positioned differently in the RCM, probably more realistically, which also has a secondary maximum in south east India. The precipitation response is more variable with increases seen over land towards the west and over the Indian ocean and decreases over much of the rest of the domain. The response of other surface variables (soil moisture, runoff, evaporation) is coupled to the temperature and precipitation anomalies.

In the GHG experiments, the active/break cycle intensifies in the sense of more, longer lasting periods of each regime. This is consistent with an increase in monsoon intensity implied by a larger mean pressure difference between the Mascarene high and the monsoon trough. Mean departures from the long term mean in both low level flow and precipitation diminish during active and break periods. The clear relative spatial differences between active and break precipitation regimes, however, undergo little change, but mean break precipitation over southern India is now similar to the full mean in both models. In the RCM this feature probably results from a diminished reduction in the strength of the break period low level jet. The GCM's response in these aspects is suspect due to its poor control behaviour.

These results are consistent with previous work (Bhaskaran *et al.*, 1998), which has shown that the regional model is capable of developing observed circulation features not present in the GCM. In the current study, the RCM has demonstrated its ability to simulate climatic features (active/break regimes) with a superior skill to its driving model whilst not deviating from the GCM's long term mean large scale circulation. A full understanding of the physical mechanisms behind the contrasting RCM and GCM behaviour and their responses to climate change has not been attempted here. A more comprehensive study of the break and active composites of other circulation and surface variables will be required to explain the different GCM and RCM behaviour. Reasons for the different responses in surface climatology, and the degrees of confidence which may be attributed to them, will follow from ongoing analysis and will be reported in a future publication.

Bibliography

Alekseeva, L. I., Semenov, E. K., and Petrosyants, M. A. 1989 Typical air flow patterns for different phases of the Indian monsoon. *Soviet Meteorology and Hydrology*, (2).

Annamalai, H., Slingo, J. M., Hodges, K., Rupakumar, K., and Tschuck, P. 1998 *SHIVA Atlas: Climatology of the Asian Summer Monsoon from ECMWF Reanalyses and Analyses for the AMIP II period (1979-95). Available from the Centre for Global Atmospheric Modelling, University of Reading, UK.*

Bhaskaran, B. and Mitchell, J. F. B. 1998 Simulated changes in southeast Asian monsoon precipitation resulting from anthropogenic emissions. *International Journal of Climatology*, **18**, 1455–1462.

Bhaskaran, B., Mitchell, J. F. B., Lavery, J., and Lal, M. 1995 Climatic response of the Indian subcontinent to doubled CO_2 concentrations. *Int. J. Climatol.*, **15**, 873–892.

Bhaskaran, B., Jones, R. G., Murphy, J. M., and Noguer, M. 1996 Simulations of the Indian summer monsoon using a nested regional climate model: domain size experiments. *Clim. Dyn.*, **12**, 573–587.

Bhaskaran, B., Murphy, J., and Jones, R. 1998 Intraseasonal oscillation in the indian summer monsoon simulated by global nested regional climate models. *Monthly Weather Review*, **126**(12), 3124–3134.

Blackmon, M. L. 1976 A climatological spectral study of the 500 mb geopotential height of the northern hemisphere. *J. Atmos. Sci.*, **33**, 1607–1623.

Cadet, D. 1983 The monsoon over the Indian ocean during summer 1975. Part II: Break and active monsoons. *Monthly Weather review*, **111**, 95–108.

Chakraborty, B. and Lal, M. 1994 Monsoon climate in a doubled CO_2 atmosphere as simulated by CSIR09 model. *TAO*, **5**(4), 515–536.

Frei, C. and Shär, C. 1998 A precipitation climatology of the Alps from high-resolution rain-guage observations. *International Journal of Climatology*, **18**, 873–900.

Gibson, J. K., Kallberg, P., Uppala, S., Hernandez, A., , Nomura, A., and Serrano, E. 1997 ERA description. ECMWF Re-anlysis Project Report Series 1, European Centre for Medium Range Weather Forecasts.

Giorgi, F. 1990 Simulation of regional climate using a limited area model nested in a general circulation model. *Journal of Climate*, **3**(9).

Goswami, B. N. 1998 Interannual variations of Indian summer monsoon in a GCM: External conditions versus internal feedbacks. *Journal of Climate*, **11**, 501–522.

Hamilton, M. G. 1977 Some aspects of break and active monsoon over southern Asia during summer. *Tellus*, **29**(4), 335–344.

Hamilton, M. G. 1979 Aspects of tropospheric structure over the bay of bengal during active and break monsoon over india in august 1977. *The Meteorological Magizine*, **108**(1286), 253–260.

IMD 1943 Climatic charts of India and neighbourhood for meteorologists and airmen. India Meteorological Department.

Johns, T. C., Carnell, R. E., Crossley, J. F., Gregory, J. M., Mitchell, J. F. B., Senior, C. A., Tett, S. F. B., and Wood, R. A. 1997 The second Hadley Centre coupled ocean-atmosphere GCM: Model description, spinup and validation. *Climate Dynamics*, **13**, 103–134.

Jones, R. G., Murphy, J. M., and Noguer, M. 1995 Simulation of climate change over Europe using a nested regional–climate model. I: Assessment of control climate, including sensitivity to location of lateral boundaries. *Q. J. R. Meteorol. Soc.*, **121**, 1413–1449.

Legates, D. R. and Willmott, C. J. 1990 Mean seasonal and spatial variability in gauge corrected, global precipitation. *Int. J. Climatol.*, **10**(2), 111–127.

Meehl, G. A. and Washington, W. M. 1993 South Asian summer monsoon variability in a model with doubled atmospheric carbon dioxide concentration. *Science*, **260**, 1101–1104.

New, M., Hulme, M., and Jones, P. 1997 Representing twentieth century space-time climate variability. I: Development of a 1961-1990 mean monthly terrestrial climatology. Submitted to Journal of Climate.

Pant, G. B. and Rupa Kumar, K. 1997 *Climates of South Asia*. John Wiley and Sons.

Rodwell, M. J. 1997 Breaks in the asian monsoon: The influence of southern hemisphere weather systems. *Journal of Atmospheric Sciences*, **54**(22), 2597–2611.

Stephenson, D. B., Chauvin, F., and Royer, J. 1998 Simulation of the Asian summer monsoon and its dependence on model horizontal resolution. *Journal of the Meteorological Society of Japan*, **76**(2), 237–265.

Webster, P. J., Magaña, V. O., Palmer, T. N., Shukla, J., Tomas, R. A., Yanai, M., and Yasunari, T. 1998 Monsoons: Process, predictability, and the prospects for prediction. *Journal of Geophysical Research*, **103**(C7), 14451–14510.

Xie, P. and Arkin, P. A. 1997 Global precipitation: A 17-year monthly analysis based on guage observations, satelite estimates and numerical model outputs. *Bulletin of the American Meteorogical Society*, **78**(11), 2539–2558.